J Indian Inst Sci., Sept.–Oct 1996, **76**, 543–553.

Structure and dynamics by resonance Raman spectroscopy

G. M. HEGDE, R. ANANDHI, G. BALAKRISHNAN, N. BISWAS AND S. UMAPATHY*
Department of Inorganic and Physical Chemistry, Indian Institute of Science, Bangalore 560 012, India.

Received on May 4, 1995; Revised on January 29, 1996

Abstract

In the present paper, the use of resonance Raman and time-resolved resonance Raman spectroscopy to understand the structure and chemical dynamics has been explained briefly along with the experimental setup. A brief theoretical analysis of resonance Raman intensities which facilitates an understanding of molecular vibrational displacements is also provided.

Keywords: Resonance Raman spectroscopy, chemical dynamics, molecular vibrational displacement

1. Introduction

Raman spectroscopy is a powerful technique to study vibrational motion in molecules. In recent years, there has been considerable interest in the use of Raman spectroscopy not only to understand the structural properties but also to study the dynamics in the excited states. Spontaneous Raman scattering is a weak process and therefore the resonance Raman (RR) effect is invariably used to study the structure of the molecules. But for certain disadvantages in the RR process, *viz.*, (i) only selective chromophores in a given molecular structure can be studied, and (ii) interferences of the fluorescence due to electronic excitation in resonance, this technique has a multitude of advantages. In particular, the Raman scattering cross section is increased by orders of magnitude (10^6–10^4) on resonance, thus resulting in an intense Raman spectrum. This is particularly useful if one is looking at species present in very low concentrations, for example, radical intermediates and excited states. Further, the RR technique can be utilised to monitor the change in the structure of the chromophore of interest as it undergoes either a chemical reaction or structural alterations such as isomerization or rearrangement.

These observations of changes in structure, through RR with appropriate time resolution, facilitate the study of dynamics associated with the process. In this paper we look at time ranges from nanoseconds (ns) to femtoseconds (fs) with particular emphasis on photoinitiated processes. In the case of the ns and picosecond (ps) processes one can use two laser pulses having appropriate time resolution, one to photoexcite the molecule to initiate the photochemical and photophysical processes and the other to probe the RR scattering of the intermediate state involved. In this regard, the experimental setup and

*Author for correspondence.

the related research being carried out in the nanosecond time domain in our laboratory are presented in subsequent sections.

In the case of the fs time scale process, due to constraints forced by the uncertainty principle, it is not possible to resolve the vibrational structure with fs pulses (having Fourier transform limited linewidth of a few tens of wavenumbers). Therefore, one can resort to theoretical analysis of the RR intensities which provides a simple and tractable method to understand molecular vibrational displacements in the fs time domain. This approach to dynamics is also presented in the last section of this paper with emphasis on the work being carried out in our laboratory.

2. Experimental

The experimental setup and measurement procedures used in resonance and time-resolved resonance Raman (TR^3) studies have been discussed previously in detail in sev-

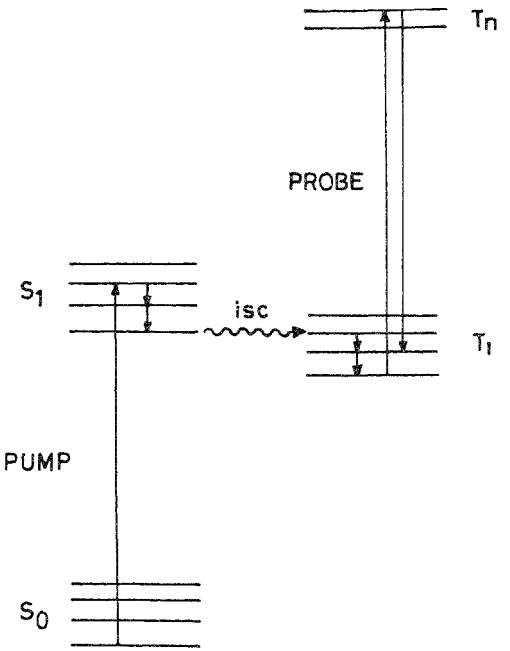

FIG 1. Schematic diagram of the pump–probe dynamics.

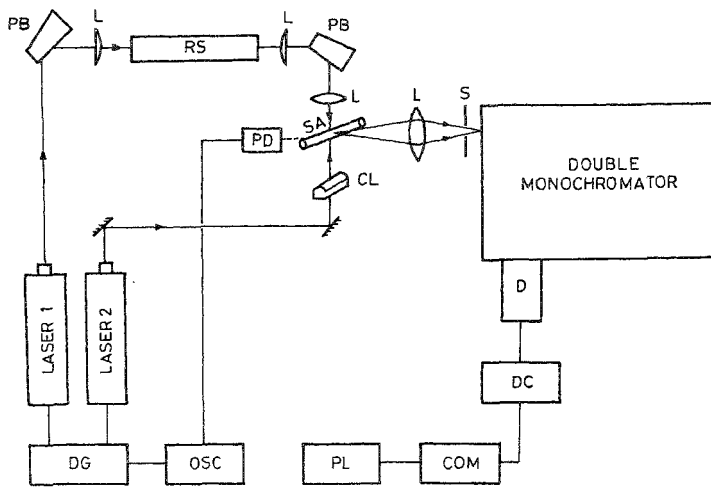

FIG. 2 Block diagram of the experimental setup used for TR[3] spectroscopy. PB:Pellin broca prism, L:Lens, SA:Sample, S:Slit, CL Cylindrical lens, PD:Photodiode, DG Delay generator, OSC:Oscilloscope, D:Detector, DC Detector controller, COM:Computer, and PL:Plotter.

eral review articles and papers[1-3]. In a typical TR[3] experiment (Fig. 1), one uses two laser beams; one (pump) tuned into an absorption of the ground state of the molecule (S_0) to create the transient state and the other (probe) tuned into an absorption band of either the excited state (T_1) or the intermediate state of interest in order to record its resonance enhanced Raman spectrum. The time delay (Δt) between the pump and the probe pulses is varied such that the time-dependent resonance Raman spectrum can be recorded at various time delays.

A block diagram of the experimental setup used for ns TR[3] spectroscopy is presented in Fig. 2. The system is based on two Q-switched ns-pulsed ND:YAG lasers (Quanta Ray DCR-11, 10 Hz repetition rate, 8 ns pulse duration) with frequency doubled and tripled output. The third (355 nm) and fourth (266 nm) harmonics are used mainly for pumping, while the second harmonic (532 nm) from the second laser is used for probing. Also, by using a locally fabricated H_2 gas Raman shifter, other wavelengths, *viz.*, 683 and 436 nm from 532 nm input and 416, 503 and 634 nm from 355 nm input, are generated. The Raman shifter is made using a 50-cm-long stainless steel tube having 5 cm inner diameter and 1 cm thickness. Both ends of the tube are closed with glass/quartz windows and the hydrogen gas was filled to a pressure of 12 bar. In Fig. 3, the input and output energies of the locally fabricated Raman shifter are shown as an indication of its

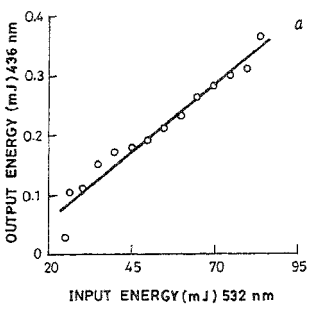

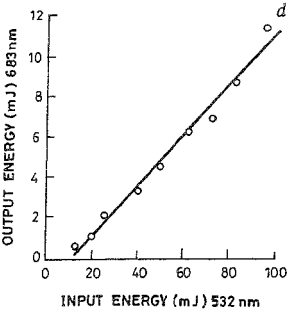

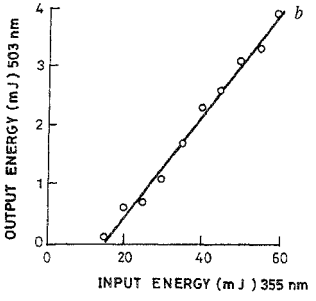

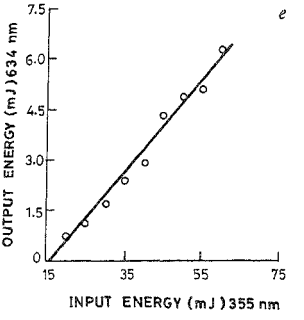

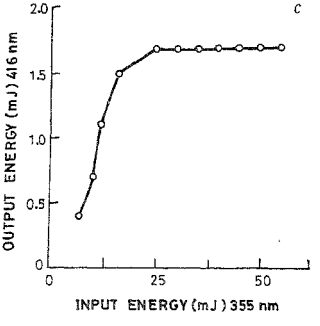

FIG. 3. Performance of the Raman shifter for 355 and 532 nm input.

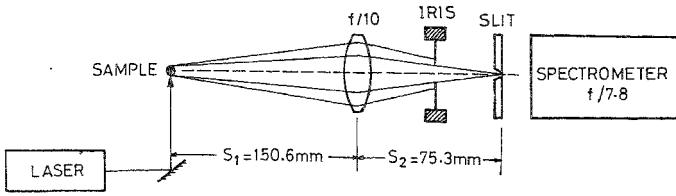

FIG. 4. Optical diagram of the collection optics

performance. The selection of the wavelengths for pumping and probing are made based on the ground and transient state absorption data of the system under study. Both pump and probe beams are focussed and spatially superimposed on the sample solution kept in the glass/quartz capillary of 2 mm internal diameter. Static or flowing sample technique is employed depending upon the photostability of the system. Flowing jet or spinning sample technique can also be used in TR^3 spectroscopy to avoid dielectric breakdown and local heating.

Both pump and probe beams are focussed on the sample either in 180° configuration or collinearly. The Raman scattering collected by a camera lens (Nikon) at an angle of 90° with respect to excitation pulse is imaged on to the entrance slit of the monochromator (SPEX 1404, 600 grooves/mm grating blazed to 500 nm). Since the camera lens cannot be used for UV excitation, a biconvex lens-based collection optics has been designed and implemented (Fig. 4). The Raman signals are detected using charge-coupled devices (CCD). For a TR^3 experiment, intensified CCD is preferred wherein one can electronically gate the detector to avoid signals generated by the pump laser. The time delay between the pump and probe pulses is monitored on the digital oscilloscope (HP-54520A) through a photodiode (ET2010). The delay is varied using a delay generator (DG535; Stanford Research Systems) which controls the two lasers. Data collection and processing are done using a computer (AT286) through detector controller (ST130; Princeton Instruments).

3. Research problems addressed

3.1. *Model compounds for photoconducting polymers*

The potential use of organic polymers in light-sensitive devices and low-cost photovoltaic cells has stimulated interest in their electronic and excited state structural properties. Among these, polyvinyl carbazole (PVCZ) has been widely investigated because of its technical importance as a photoconductor. The charge carrier that is responsible for photoconduction in doped PVCZ has been found to be the radical cation of PVCZ[4]. The mechanism of formation of this radical cation from the excited state produced by photoexcitation has been studied to date by transient absorption spectroscopy in the presence or absence of electron acceptors. In order to understand the structural details of the radical cation, TR^3 spectroscopy has been used to study the vibrational structure. Raman

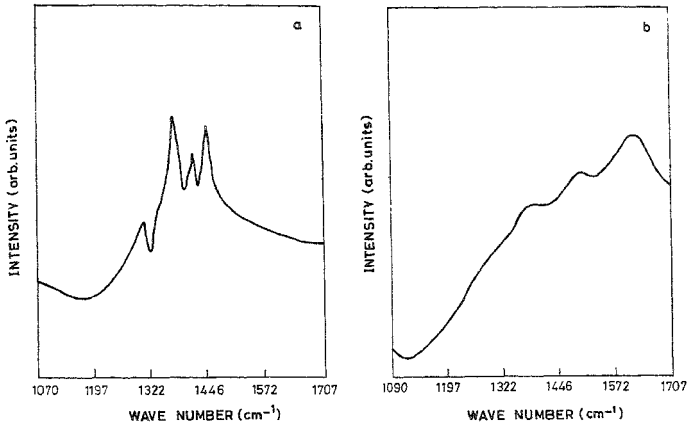

FIG. 5. Raman spectrum of (a) Dibromo-N-ethyl carbazole monomer radical cation, and (b) N-ethyl carbazole dimer radical cation ($\lambda_{exc} = 416$ nm).

spectroscopic studies of radical cations formed either by chemical means or by electrochemical methods are required to compare with the TR[3] spectrum.

As *a priori*, we study the model compound, N-ethyl carbazole (NEC). This would be an ideal starting point since its electronic and spectroscopic properties have been found to be very similar to that of PVCZ. NEC can be oxidized to its radical cation by ceric ammonium nitrate and perchloric acid. It is known that NEC cation can dimerize to 3,3′, N-ethyl bicarbazolyl dimer dication salt[5]. In order to prepare stable nondimerizable radical cation, active dimerizing sites have to be blocked. This is achieved by brominating NEC to 3,6-dibromo, NEC (DBNEC)[6]. DBNEC has been oxidized to the monomer radical cation of DBNEC by ceric ammonium nitrate and perchloric acid. Spectroscopic studies for radical cation of DBNEC and dimer dication of NEC are in progress.

In order to understand the structural details, RR spectra of these radicals have been recorded (Fig. 5). These differ considerably indicating the changes in the structure of these intermediates. A comparison and analysis of RR data of monomer and dimer radical cations with PVCZ radical cations would give further information on its structure.

3.2. *Biologically relevant quinones*

Quinones widely occur in nature and their photophysical and photochemical properties are of interest[7]. Among various quinones, menadione (2-methyl-1,4-napthoquinone) constitutes the basic skeleton of several quinones (Vitamin K series) which are of importance in many biochemical processes such as the transport of electrons to cytochrome. In

the triplet state, it acts as a sensitizer in the oxidation of nucleic acid bases. The photochemistry and photophysics of menadione involves various intermediates such as triplet states, radical anions and semiquinone radicals. Photoexcitation of aqueous menadione in the presence of oxygen and different electron donors causes various reactions following the formation of triplet menadione(^{3}MQ) from the singlet menadione(^{1}MQ). Fischer and Land[8] proposed a mechanism from their flash photolysis studies as shown.

$$\text{MQ} \rightarrow {}^1\text{MQ} \rightarrow {}^3\text{MQ} \begin{cases} \xrightarrow{2\text{H}_2\text{O}} \text{MQ} + \text{MQ}^{\cdot-} + \text{OH}^* + \text{H}_3\text{O}^+ \\ \text{2 MQ self-quenching} \\ \\ \text{MQ} + {}^1\text{O}_2 \text{ energy transfer only} \\ \text{MQ}^{\cdot-} + \text{D}^{\cdot-} \text{ electron transfer} \end{cases}$$

The triplet decays spontaneously to ground state menadione with the formation of small amounts of menadione semiquinone anion radical($MQ^{\cdot-}$). It has also been suggested that the direct abstraction of hydrogen atom from water leads to the formation of semiquinone radical (MQH). This MQH then dissociates to an anion radical ($MQ^{\cdot-}$)[8]. The direct reactions of triplet menadione with water are not clear and the present study is focussed on this aspect to explore the detailed mechanistic pathways for the aqueous menadione photochemistry.

$$^3\text{MQ} + \underset{\sim}{\text{H}_2\text{O}} \rightarrow \text{MQH}^{\cdot} + \text{OH}^*;$$

$$\text{MQH} \Leftrightarrow \text{MQ}^{\cdot-} + \text{H}^+ \text{ (pKa 4.6)}.$$

Flash photolysis and pulse radiolysis techniques have been used to identify the various intermediates involved in menadione aqueous photochemistry[9-13]. The ground state has absorption bands at 264 nm ($\pi - \pi^*$) and 330 nm ($n - \pi^*$). On excitation around 350 nm, menadione forms triplet states from singlet states through intersystem crossing. Quantum yield of the triplet state was found to be 0.66. The triplet has an absorption maximum centered at 390 nm extending to 500 nm, with lifetime in the sub-μs time scale (decay rate constant 1.1×10^{-7} s^{-1}). The decay rate depends on various factors such as the presence of electron donors, oxygen and menadione concentration. The radical anion has an absorption maxima at 395 and 300 nm with ε values of 1.2×10^4 and 1.25×10^4 M^{-1} cm^{-1}, respectively. The semiquinone radical absorbs at 370 and 290 nm with ε values 9.5×10^3 and 6×10^3 M^{-1} cm^{-1}, respectively. Both flash photolysis and pulse radiolysis are powerful tools in the identification of these intermediate species and in the study of their kinetics. The absorption spectra of a species in solution usually consists of broad bands revealing little or no information about the structure which is necessary for detailed understanding of their architecture and the nature of the chemical bonding within them. As TR^3 spectroscopy is a powerful structure-sensitive technique, these reactive intermediates can be studied using this technique.

In spite of various studies on the menadione photochemistry and photophysics, structural information about the various intermediates is still scant. Since the reaction of these intermediates with various substrates determines their function, a systematic study of menadione photochemistry and photophysics is very important. In order to understand the structure–function relationships in these intermediates, we have undertaken a TR^3 spectroscopic study. Experiments in different environments (like various solvents, at different PH, in the presence of various donors, etc.) can be carried out to understand the fundamental aspects of electron transfer reactions in solution. Such a study would lead to a better understanding of the structure of intermediates and its implications on reactivity.

The TR^3 spectra of menadione (1.5×10^{-3} M) in water does not show any detectable amount of transient signal. $NaNO_2$ is known to act as a very good electron donor for triplet aromatic compounds and in the case of menadione, it reacts with the triplet and forms a semiquinone anion radical[13]. The TR^3 spectra of menadione (1.5×10^{-3} M) in water in the presence of $NaNO_2$ (0.1 M) is shown in Fig. 6. The pump and probe laser wavelengths are 355 (2 mJ) and 416 nm (1 mJ), respectively, and the time delay between the pump and probe laser is 20 ns. One intense band was observed at 1602 cm^{-1} which decays over a period of a few hundred nanoseconds. This band is assigned to a coupled motion of C=C and C=O stretching frequency of the anion radical. *Ab-initio* quantum mechanical calculations were carried out on the neutral and anion radical of the menadione to support the experimental data. Currently work is in progress to confirm our present results and to characterize the other intermediates involved in menadione photochemistry.

3.3. *Dynamics from resonance Raman intensities*

An analysis of the Raman intensities of various vibrational modes observed under resonance would provide information on the architectural changes associated with the given excitation. In particular, a comparison of the theoretically calculated Raman excitation profile (REP) with that of the experimental spectrum would provide vital clues regarding the dynamics involved with a specific vibrational mode[14,15]. Heller's wavepacket propagation technique[16–19] can be used to simulate the absorption and REPs for various vibrational modes of a given system. Accurate knowledge of the normal modes can give us an idea of the dynamics associated with the system under study in the early femtosecond time scale. In the present study, the time-dependent quantum mechanical (TDQM) method involving grid technique[20,21] has been used for propagation of wavepackets on the excited state surface. In order to test its validity, the TDQM approach has been applied to polyatomic systems such as *cis*-stilbene which was semiclassically studied previously by Myers and Mathies[14,15].

A detailed discussion of the theoretical method has been presented elsewhere[22]. However, briefly, in the time-dependent picture the initial wavepacket $|i>$ corresponding to the ground, electronic and vibrational state is transferred to the electronically excited state where it starts moving under the influence of the excited state Hamiltonian (H_{e1}). This wavepacket $|i(t)>$ moves away from the Franck–Condon region in time t. The moving wavepacket can then be overlapped with various vibrational levels $|f>$ or $|f>$ of the ground electronic state (where $|f>$ corresponds to the ground electronic first vibrational

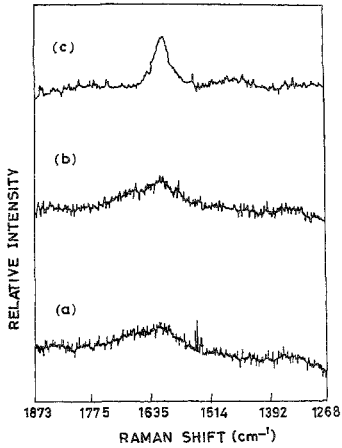

FIG. 6. TR[3] spectrum of aqueous menadione (1.5×10^{-3}) in the presence of $NaNO_3$ (0.1 M). (a) probe only, and (b) pump and probe and (c) (a)–(b)

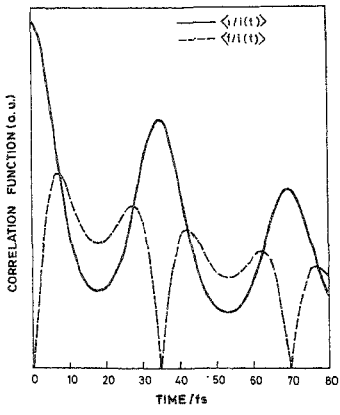

FIG. 7 The autocorrelation function $\langle i|i(t)\rangle$ (solid line) and correlation function $\langle f|i(t)\rangle$ (dashed line) for H_{oop} mode with frequency $\omega = 963\ cm^{-1}$

state), thus leading to autocorrelation $\langle i|i(t)\rangle$ and correlation $\langle f|i(t)\rangle$ functions. The full and half Fourier transformation of the autocorrelation and correlation functions multiplied by the damping factor, $\exp(-\Gamma t/\hbar)$, where Γ is the homogeneous broadening, gives the absorption (σ_A) and the Raman (σ_R) amplitudes, respectively.

$$\sigma_A(E_L) = \frac{4\pi e^2 M^2 E_L}{6\hbar^2 cn} \int_{-\infty}^{+\infty} \langle i|i(t)\rangle \exp\left(i(E_L + E_i)t/\hbar - \Gamma|t|/\hbar\right) dt \tag{1}$$

$$\sigma_R(E_L) = \frac{8\pi e^4 M^4 E_s^3 E_L}{9\hbar^6 c^4} \left| \int_0^{\infty} \langle f|i(t)\rangle \exp\left(i(E_L + E_i)t/\hbar - \Gamma|t|/\hbar\right) dt \right|^2 \tag{2}$$

where e is charge of the electron, c, the velocity of light, n, the refractive index of the solution, $\hbar = h/2\pi$ (h being Planck's constant), M, the electronic transition moment, E_L, the energy of the incident photon, E_i, zero point energy of the ground electronic state, E_s, energy of the scattered radiation, and $|i(t)\rangle = \exp(-iH_{ex}t/\hbar)|i\rangle$.

For *cis*-stilbene the autocorrelation function $\langle i|i(t)\rangle$ and correlation function $\langle f|i(t)\rangle$ for the H_{oop} (out-of-plane wag) with frequency $\omega = 963\ cm^{-1}$ has been simulated (Fig. 7). The product autocorrelation function for the ethylenic C = C stretching ($\omega = 1629\ cm^{-1}$) and that of $\omega = 963\ cm^{-1}$ mode is given in Fig. 8. The simulated absorption spectrum of *cis*-stilbene is shown in Fig. 9. A comparison of the simulated results with those of Myers' work[15] shows that the TDQM technique provides accurate results similar to that obtained from semiclassical techniques, thus demonstrating the viability of the TDQM

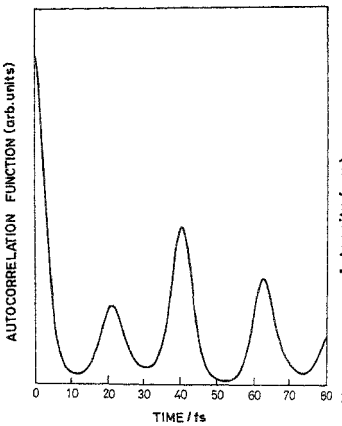

FIG 8. Product autocorrelation function for ethylenic C = C stretching ($\omega = 1629$ cm^{-1}) and H_{out} ($\omega = 963$ cm^{-1}) modes.

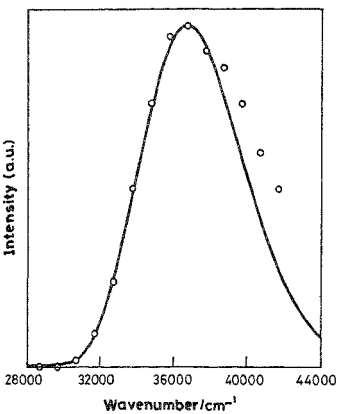

FIG 9 Simulated (—) and experimental (o) absorption spectrum of *cis*-stilbene.

approach to these problems. Further work is in progress to study the dynamics associated with systems undergoing isomerization under resonance excitation (*i.e.*, to study the changes in internal coordinates for the specific vibrational modes at various times upon excitation).

4. Conclusion

In this paper, we have provided a brief outline of the research objectives in our research group. The utility of TR^3 spectroscopy and RR intensity analysis has been presented along with a description of the experimental setup used for such experiments. Further, various research problems that are investigated using the above techniques have been discussed to provide a glimpse of the kind of specific questions that can be addressed using TR^3 and RR spectroscopy.

Acknowledgements

We thank the Jawaharlal Nehru Centre for Advanced Scientific Research, Bangalore, and the Indian Institute of Science for facilities, and the CSIR and DST for partial financial support.

References

1. PAGSBERG, G., WILBRANT, R., HANSEN, K. V. AND WEISBERG, C. V. Fast resonance Raman spectroscopy of short-lived radicals, *Chem Phys. Lett*, 1976, **39**, 538.

2. ATKINSON, G. H. — In *Advances in infrared and Raman spectroscopy*, Vol. 9 (R. J. H. Clark and R. E. Hester, eds), 1981, Wiley.

3. HAMAGUCHI, H. — In *Vibrational spectra and structure*, Vol. 16 (J. R. Durig, ed.), 1987, Elsevier.

4. WILLINGHOFF, S. T., THOMAS, K. J., AND DICK, J. S. — Electronic conduction mechanism in polycarbazole iodine complex, *Mol Cryst Liq. Cryst.*, 1984, **106**, 289.

5. AMBROSE, J. G. AND NELSON, R. F. — Anodic oxidation pathways of carbazoles, *J Electrochem Soc.*, 1958, **115**, 1159.

6. AMBROSE, J. G. AND NELSON, R. F. — Electrochemical and spectroscopic properties of cation radicals, *J. Electrochem. Soc.*, 1976, **122**, 876.

7. MORTON, R. A. — In *Biochemistry of quinones*, 1965, Academic Press.

8. FISCHER, J. AND LAND, J. — Photosensitization of pyrimidines by 2-methylnaphthoquinone in water, *Photochem. Photobiol.*, 1983, **37**, 27.

9. PATEL, K. B. AND WILSON, R. L. — Semiquinone free-radicals and oxygen, *J Chem. Soc Faraday Trans.*, 1973, **69**, 8.

10. HAYON, E. AND SIMIC, M. — Addition of hydroxyl radicals to pyrimidine bases and electron transfer reactions of intermediates to quinones, *J. Am Chem. Soc.*, 1973, **95**, 1029.

11. RAO, P. S. AND HAYON, E. — Ionization constants and spectral characteristics of some semiquinone radicals in aqueous solution, *J. Phys Chem.*, 1973, **77**, 2274.

12. RAO, P. S. AND HAYON, E. — One-electron redox reactions of free radicals in solution: Rate of electron transfer processes to quinones, *Biochem. Biophys. Acta*, 1973, **292**, 516.

13. LOEFF, I., GOLDSTEIN, S., TREININ, A. AND LINSCHITZ, H. — Interaction of formate ion with triplets of anthraquinone-2-sulphonate, 1,4-naphthbenzophenone-4-carboxylate, and benzop-4-sulfonate, *J Phys. Chem.*, 1991, **95**, 4423.

14. MYERS, A. B. AND MATHIES, R. A. — Resonance Raman intensities A probe of excited structure and dynamics. In *Biological applications of Raman spectroscopy* (T. G. Spiro, ed.), Vol. 2, 1987, Wiley.

15. MYERS, A. B. AND MATHIES, R. A. — Excited-state torsional dynamics of *cis*-stilbene from resonance Raman intensities, *J. Chem Phys.*, 1984, **81**, 1552.

16. HELLER, E. J. — The semiclassical way to molecular spectroscopy, *Acct Chem. Res.*, 1981, **14**, 368.

17. HELLER, E. J., SUNDBERG, R. L. AND TANNOR, D. J. — Simple aspects of Raman scattering, *J. Phys. Chem.*, 1982, **86**, 1822.

18. LEE, S. Y. AND HELLER, E. J. — Time-dependent theory of Raman scattering, *J. Chem. Phys.*, 1979, **71**, 4777.

19. TANNOR, D. J. AND HELLER, E. J. — Polyatomic Raman scattering for general Harmonic potentials, *J. Chem. Phys.*, 1982, **77**, 202.

20. KOSLOFF, R. — Time-dependent quantum mechanical method for molecular dynamics, *J. Phys. Chem.*, 1988, **92**, 2087.

21. WILLIAMS, S. O. AND IMRE, D. G. — Raman spectroscopy: time dependent pictures, *J. Phys. Chem.*, 1988, **92**, 3363.

22. BISWAS, N., UMAPATHY, S., KALYANARAMAN, C. AND SATHYAMURTHY, N. — Raman intensity analysis of polyatomic molecules, *Proc. Indian Acad. Sci (Chem. Sci.)*, 1995, **107**, 233.